# Identification of an isoflavonoid transporter required for the nodule establishment of the *Rhizobium-Fabaceae* symbiotic interaction

Wanda Biała-Leonhard[1]†, Laura Zanin[2]†, Stefano Gottardi[2]†, Rita de Brito Francisco[3], Silvia Venuti[2], Fabio Valentinuzzi[2,4], Tanja Mimmo[4], Stefano Cesco[4], Barbara Bassin[3], Enrico Martinoia[3], Roberto Pinton[1], Michał Jasiński[1,5*], Nicola Tomasi[2*]

[1]Department of Plant Molecular Physiology, Institute of Bioorganic Chemistry, Polish Academy of Sciences, Noskowskiego 12/14, 61-704 Poznań, Poland.

[2]Dipartimento di Scienze Agro-Alimentari, Ambientali e Animali, University of Udine, Via delle Scienze 206, 33100 Udine, Italy.

[3]Institute of Plant and Microbial Biology, University of Zurich, Zollikerstrasse 107, 8008 Zurich, Switzerland.

[4]Faculty of Science and Technology, Free University of Bozen Bolzano, Piazza Università 5, 39100 Bolzano, Italy.

[5]Department of Biochemistry and Biotechnology, Poznań University of Life Sciences, Dojazd 11, 60-637 Poznań, Poland.

†These authors contributed equally

*To whom correspondence should be addressed: Nicola Tomasi, Email: nicola.tomasi@uniud.it, Phone: +39 0432 558637; Michał Jasiński, Email: jasinski@ibch.poznan.pl , Phone: +48-61-852-85-03

## SUMMARY

Nitrogen (N) as well as Phosphorus (P) are key nutrients determining crop productivity. Legumes have developed strategies to overcome nutrient limitation by e.g., forming a symbiotic relationship with N-fixing *rhizobia* and the release of P-mobilizing exudates and are thus able to grow without supply of N or P fertilizers. The legume-rhizobial symbiosis starts with root release of isoflavonoids, that act as signaling molecules perceived by compatible bacteria. Subsequently, bacteria release nod factors, which induce signaling cascades allowing the formation of functional N-fixing nodules.

We report here the identification and functional characterization of a plasma membrane-localized MATE-type transporter (LaMATE2) involved in the release of genistein from white lupin roots.

The *LaMATE2* expression in the root is upregulated under N deficiency as well as low phosphate availability, two nutritional deficiencies that induce the release of this isoflavonoid. *LaMATE2* silencing reduced genistein efflux and even more the formation of symbiotic nodules, supporting the crucial role of LaMATE2 in isoflavonoid release and nodulation. Furthermore, silencing of LaMATE2 limited the P-solubilization activity of lupin root exudates. Transport assays in yeast vesicles demonstrated that LaMATE2 acts as a proton-driven isoflavonoid transporter.

## KEY WORDS

*Bradyrhizobium*, genistein, *Lupinus albus*, MATE transporter, Nitrogen, Phosphorus, plant-microbe interaction

## INTRODUCTION

One of the major challenges of sustainable agriculture comprises the production of high-quality plant material with preservation of soil components and reduced application of chemical fertilizers without penalizing yield. Nitrogen (N) and phosphorus (P) are limiting nutrients in most natural soils (Tilman, 1999). High input of N-fertilizers is required to sustain crop growth in conventional agriculture. However, this feature may contaminate soils and groundwater and markedly contribute to the release of greenhouse gases (Tilman et al., 2001). Much of the P in soils is not available to plants due to its tendency to interact with calcium and magnesium salts or iron and aluminum oxides. It is mainly present as sparingly soluble rock phosphate, or it is immobilized in slowly mineralizable P-containing organic compounds, such as phytates. Phosphorous is a non-renewable resource which is mined at an increasing rate to meet the demand for fertilizers (Vance et al., 2003).

*Leguminous* plants (*Fabaceae*) such as soybean and lupin, have evolved several strategies to survive in low nutrient soils. In the case of P, in many ecosystems and, in particular, in acidic soils, the plant`s response consists mainly in the association with mycorrhizal fungi or the formation of particular root structures, such as cluster roots (Purnell, 1960; Neumann and Martinoia, 2002; Lambers et al., 2015). Cluster roots release huge amounts of exudates into the rhizosphere which are mainly composed of carboxylates and flavonoids. Flavonoids are involved both in the mobilization of nutrients and in the modulation of soil microbial activities (Cesco et al., 2010). The production and release of flavonoids, are also essential for the establishment of the symbiotic interaction between legumes and N-fixing bacteria such as *Ensifer*, *Bradyrhizobium* or *Mesorhizobium*, leading to the fixation of atmospheric N. Moreover it has been hypothesized that flavonoids are involved in the initiation

86 of the nodule through their action on the plant hormone auxin and
87 could thus play a developmental role in addition to their action as
88 nod gene regulators (Subramanian et al., 2006; Wasson et al., 2006;
89 Li et al., 2016).
90 The mutualistic fungal and bacterial symbionts are striking
91 examples of soil microorganisms that have successfully coevolved
92 with their hosts since plants adapted to terrestrial ecosystems. They
93 promote plant growth by facilitating the acquisition of scarce
94 nutrients. The most commonly established symbiosis in plants is the
95 mycorrhizal association, with 80–90% of all land-plant species able
96 to enter this interaction. Around 100 Mio years ago, certain
97 angiosperms evolved a bias toward the evolution of nodulation with
98 the so-called N-fixing soil bacteria. Among those angiosperms are
99 legumes (*Fabales*) and one non-legume genus, *Parasponia*
100 (*Cannabaceae*, *Rosales*) which can establish mutualistic symbioses
101 with *Rhizobia*, a polyphyletic group of proteobacteria and diverse
102 group of plants belonging to the orders *Fagales*, *Rosales*, and
103 *Cucurbitales* which can associate symbiotically with filamentous
104 actinobacteria of the genus *Frankia* (Martin et al., 2017). By
105 forming symbiotic associations, plants obtain mineral nutrients. In
106 turn, they supply the symbiont with organic compounds, sugars and
107 lipids in the case of mycorrhiza, mostly carboxylates to N-fixing
108 bacteria (Udvardi and Poole, 2013; Jiang et al., 2017; Luginbuehl et
109 al., 2017). The establishment of the symbiosis is a complex event
110 and requires coordinated regulation of the corresponding genes and
111 release of signaling molecules into the rhizosphere. For the legume-
112 *rhizobia* symbiosis, it is expected that a flavonoid transporter must
113 be present in the plasma membrane of root cells to release
114 isoflavonoids into the rhizosphere (Sugiyama et al., 2007). Up to
115 now, transporters for flavonoids have been mainly described at the
116 vacuolar membrane (Zhao, 2015). Furthermore, an ABC (ATP-

117 Binding Cassette) transporter from *Medicago* was shown to
118 transport flavonoids. However, this transporter is localized in the
119 vasculature (Biala et al., 2017). Using a biochemical approach
120 Sugiyama and coworkers (2007) presented evidence that, in
121 soybean, genistein transmembrane transport is mediated by an
122 ABC-type transport system. But its contribution to genistein root
123 release and the legume-*rhizobia* symbiosis establishment is still
124 unclear.
125 Despite all the research performed on this symbiotic interaction, a
126 transporter releasing flavonoids into the rhizosphere and initiating
127 the first step of this symbiosis awaits its identification.
128
129
130 **MATERIALS AND METHODS**
131 **Plant growth and transformation**
132 White lupin seeds (*Lupinus albus* L. cv. Amiga; Südwestdeutsche
133 Saatzucht, Rastatt, Germany) were soaked for 24 hours in aerated
134 water and germinated on a plastic net placed at the surface of an
135 aerated 0.5 mM $CaSO_4$ solution in a growth chamber at 25 °C in the
136 dark. Thereafter, 7-day-old seedlings were transferred to a
137 hydroponic system, containing a P-free nutrient solution (µM): 5000
138 $Ca(NO_3)_2$, 1250 $MgSO_4$, 1750 $K_2SO_4$, 250 KCl, 20 Fe(III)EDTA,
139 25 $H_3BO_4$, 1.25 $MnSO_4$, 1.5 $ZnSO_4$, 0.5 $CuSO_4$, 0.025
140 $(NH_4)_6Mo_7O_4$. Phosphorus-deficient plants were grown on P-free
141 nutrient solution, while 0.25 mM $KH_2PO_4$ were added to nutrient
142 solution for P-sufficient condition. Plants were grown under
143 controlled conditions for 4 weeks (day/night photoperiod, 16/8 h;
144 radiation, 220 µE $m^{-2}s^{-1}$; day/night temperature, 25/20 °C; relative
145 humidity, 70-80%).
146

147 In P-deficiency, lupin plants modify the root architecture developing
148 particularly root structures, called cluster roots or proteoid roots. In
149 order to differentiate the developmental stages of root clusters
150 (Figure S1), the root system was immerged in a pH-indicator
151 solution (0.04% w/v bromocresol purple). Depending on their
152 morphology and capability to acidify the solution, at the end of the
153 growing period different regions of cluster root were sampled from
154 P-deficient plants (juvenile, immature, mature, senescent), as
155 described by Massonneau and coworkers (2001). Root apices and
156 cluster root parts were sampled from a pool of 12-16 P-sufficient
157 and P-deficient plants. The samples were immediately frozen in
158 liquid nitrogen for the RNA extraction or were rinsed twice in 0.5
159 mM $CaSO_4$ solution and the root exudates were collected for one
160 hour in 0.5 mM $CaSO_4$ 10 mM 2-[N-Morpholino]ethanesulfonic
161 acid (MES)-KOH pH 6.0 at a ratio 1:10 W/V. The samples were
162 conserved at –80 °C until processing. Three independent
163 experiments were performed.
164
165 To investigate the plant response to N-deficiency, white lupin seeds
166 were grown for two weeks on watered Whatman paper in Petri
167 dishes and then transferred to the magenta boxes containing PFR N-
168 free solution described by Stróżycki and coworkers (2003). For N-
169 sufficient conditions $KNO_3$ (0.1 mM), $NH_4H_2PO_4$ (5 mM),
170 $Ca(NO_3)_2$ (2.46 mM) were added to the PFR medium. Plants were
171 grown for further two weeks under controlled conditions (day/night
172 photoperiod, 16/8 h; radiation, 220 $\mu E\ m^{-2}s^{-1}$; day/night temperature,
173 23/20 °C; relative humidity, 70-80 %). The samples were collected
174 at 7 and 14 days after the transfer in N-deficient condition. Two
175 biological repetition and 4/8 technical repetition were performed.
176

177 White lupin seedlings were transformed using *Agrobacterium*
178 *rhizogenes* ARqua1 strain (Quandt et al., 1993) carrying binary
179 vector pRedRoot::*LaMATE2 RNAi* or empty vector (EV) pRedRoot.
180 After germination 5 mm root tips were removed from radicles. The
181 sectioned surface was coated with *A. rhizogenes* and seedlings were
182 placed on solid Fahraeus medium supplemented with kanamycin (15
183 mg $L^{-1}$).
184
185 Nitrogen-deficient plants were grown and analyzed as described
186 above. For P-deficiency, after 3 weeks post germination, plants were
187 transferred to P-free nutrient solution (as described above). After 2
188 weeks, white lupin plants were moved in hydroponic solutions in P-
189 free nutrient solution and grown for 3 additional weeks. *LaMATE2*
190 expression analyses were performed, and root release was collected
191 as described previously on the fully developed cluster root
192 (immature, mature). Six biological replicates were performed for
193 each sample.
194
195 **Nodulation and effects of genistein exogenous addition**
196 Three-week-old lupin composite plants were transferred to the pots
197 filled with sterile perlite (0.75 L). Plants were nourished with PFR
198 N-free solution. After 2 week of N-deficiency plants were
199 inoculated with *B. japonicum* (strain UPP 133, (Stępkowski et al.,
200 2011)) and grown for further two weeks under controlled conditions
201 (day/night photoperiod, 16/8 h; radiation, 220 µE $m^{-2}s^{-1}$; day/night
202 temperature, 23/20 °C; relative humidity, 70-80 %). For
203 complementation experiments 1 h before inoculation with *B.*
204 *japonicum* plants were additionally supplemented with 1 µM
205 genistein solution. Fourteen-day post-inoculation plants were
206 removed from pots, nodules were counted for each single root, and
207 roots were collected for each plant. Afterwards all roots of single

208 plant were grounded and divided into aliquots dedicated for gene
209 expression and metabolomic analysis. Only plants revealing
210 expression of marker gene encoding fluorescent protein DsRed were
211 considered during analysis. These experiments were performed 6,
212 8 or 21.
213
214 **Mobilization of P from vivianite**
215 The vivianite suspension ($Fe_3(PO_4)_2 \cdot 8H_2O$) was prepared by mixing
216 $H_3PO_4$ with $FeSO_4 \cdot$as described by Eynard et al. (1992). A solution
217 of 0.035 M $H_3{}^{32}PO_4$ and 0.05 M $FeSO_4 \cdot 7H_2O$ were brought to pH
218 6.0 with 0.05 M KOH under stirring. A bluish suspension of
219 vivianite was obtained, after precipitation via centrifugation (8000
220 g, 10 min), the precipitate was washed (by 3 successive
221 centrifugations and decantations) with deionized water.
222 Mobilization of $PO_4^{2-}$ from Vivianite ($Fe_3(PO_4)_2 \cdot 8H_2O$) by exudates
223 after purification with the SPE methods, in order to remove
224 carboxylates, from *LaMATE2 RNAi* or empty vector (EV) pRedRoot
225 transformed P-deficient roots was performed as followed: one mL
226 of a suspension containing $^{32}$P-vivianite (70 µmol $PO_4$, specific
227 activity 60 KBq µmol$^{-1}$ P) was transferred into a dialysis tube
228 (ZelluTrans/Roth 6.0, ∅ 16mm, exclusion limit of 4÷6 kDa, ROTH)
229 and mixed with 5 mL of mobilization solution [0.5mM $CaSO_4$,
230 20mM Mes-KOH (pH 6.0), 50 µl methanol]. Thereafter, the dialysis
231 tube was transferred into continuously mixed 34 ml of mobilization
232 solution. At the beginning of the experiment, exudates
233 corresponding to the amount release for 1 hour by 1 gram of juvenile
234 cluster root tissues (Figure 1) were added to the external solution.
235 After 15, 30, 45 and 60 min, samples from the solution outside the
236 dialysis tube were collected and the amount of $^{32}$P was measured by
237 liquid scintillation counting. The $^{32}$P mobilization was estimated
238 from the difference between the $^{32}$P concentration measured in the

239 presence of the mock and in the absence of exudates and was
240 expressed as µmol P $h^{-1}$.
241
242 **Extraction and LC/MS analysis**
243 Frozen root tissue (500 mg) was grounded and extracted with 80%
244 methanol. Root exudates were extracted from the medium by SPE
245 (Solid Phase Extraction) method using octadecylosilane matrix and
246 methanol according to Staszków and coworkers (2011). Luteolin
247 was used as an internal standard. Samples were analyzed by liquid
248 chromatography-electrospray ionization tandem mass spectrometry
249 (LC/ESI/MS) using a Waters UPLC coupled with Bruker
250 micrOTOF-Q mass spectrometer. The analysis was performed in a
251 gradient mobile phase consisting of 0.5% formic acid (v/v) in water
252 (A) and 0.5% formic acid (v/v) in acetonitrile (B). The m/z range of
253 the recorded spectra was 50-1000. Analyses were performed in the
254 ion-positive mode.
255
256 **RNA extraction and cDNA synthesis**
257 RNA extractions were performed using the InviTrap Spin Plant
258 RNA Mini Kit (Stratec Molecular, Berlin, Germany) following
259 manufacturer's instructions and contaminant genomic DNA was
260 removed using 10 U of DNase I (GE Healthcare, Munich,
261 Germany). The quantity and the quality of RNA was checked using
262 a spectrophotometer, followed by a migration in a 1 % agarose gel.
263 One microgram of total RNA for each sample was retro-transcribed
264 using 1 pmol Oligo d(T)23 (Sigma Aldrich, Saint Louis, USA) and
265 10 U M-MulV RNase H (Finnzymes, Helsinki, Finland) following
266 manufacturers' instruction.
267
268 **Isolation of the *LaMATE2* sequence**

269 The partial sequence was isolated via a cDNA-AFLP approach
270 starting from RNA extracted from juvenile cluster roots which were
271 compared to mature and senescent cluster roots, for details see
272 Massonneau and coworkers (2001). The full Open Reading Frame
273 (ORF) of *LaMATE2* (*LaMATE2*$_{ORF}$) was isolated from the cDNA of
274 juvenile cluster root tissues from P-deficient plants using the 5'/3'
275 RACE Kit (2nd generation, Roche Diagnostics S.p.a., Monza, Italy)
276 following the manufacturer's instructions. *LaMATE2*$_{ORF}$ sequence
277 was cloned in pGEM-T easy vector (for primers see Table S1,
278 Promega Italia Srl, Milan, Italy) and deposited in the NCBI database
279 (KY464927).
280

281 **Gene expression analysis**

282 The reaction was performed by adding 0.1 µl of cDNA to
283 RT complete reaction mix, Fluocycle™ sybr green (20-µl final
284 volume; Euroclone, Pero, Italy). Specific primers were designed for
285 the target, the two closest homologues (www.whitelupin.fr;
286 Hufnagel *et al.*, 2020) and the housekeeping gene using Primer3
287 software (Koressaar and Remm, 2007; Untergasser et al., 2012) and
288 were synthesized by Sigma Aldrich (Table S1). Gene expression
289 analyses were performed using CFX96™ Real-Time System
290 (C1000TM Thermal Cycler, BioRad) and CFX Manager™
291 Software (v 2.0, BioRad). The two closest homologues
292 (*Lalb_Chr06g0165721, Lalb_Chr02g0145611*) have a low
293 expression in the root tissues and their expression levels is shown in
294 Figure S5. Data were normalized in respect to the transcript level of
295 the housekeeping gene (*Ubiquitin* gene, *LaUBI*) using the $2^{-\Delta\Delta CT}$
296 method (Livak and Schmittgen, 2001). The efficiency of
297 amplification was calculated using R program (version 2.9.0;
298 http://www.r-project.org/) with the qPCR package (version 1.1-8),

299 following the authors' indications (Ritz and Spiess, 2008). Six
300 biological replicates were performed for each sample.
301
302 **Genistein transport by LaMATE2 in *Saccharomyces cerevisiae***
303 **vesicles**
304 The construction of the yeast expression vector pNEV (Sauer and
305 Stolz, 1994) containing *LaMATE2*$_{ORF}$ was performed by amplifying
306 *LaMATE2*$_{ORF}$ sequence with primers having both a *NotI*-restriction
307 sites at the 5'end. The cloning of the PCR product (*LaMATE2*$_{ORF}$)
308 was performed into the *NotI* site of pNEV (pNEV::*LaMATE2*$_{ORF}$),
309 the orientation was verified by sequencing. The transformation of
310 competent yeast cells (*S. cerevisiae* YPH499 strain) was performed
311 following a standard procedure (Gietz and Woods, 2002) and
312 transformants were selected on synthetic dextrose minimal medium
313 lacking uracil (SD-Ura medium; Burke *et al.*, 2000).
314 The yeast cells, strain YPH499, were transformed with the pNEV
315 empty vector or pNEV::LaMATE2$_{ORF}$ and selected on liquid-SD
316 Ura-medium. Thereafter, cells were incubated in YPD medium for
317 30 min, collected by centrifugation, and digested with lyticase
318 (1,000 U $g^{-1}$ fresh weight cells; Sigma Aldrich), and subsequently
319 microsomal vesicles were isolated as described by Klein and
320 coworkers (2002). Transport assays were performed to study the
321 genistein transport using the rapid filtration technique with
322 nitrocellulose filters (0.45 µm pore size; Millipore, Millipore Co.,
323 Bedford, USA). The transport experiment was carried out in
324 presence of isolated vesicles, transport buffer (0.4 M glycerol, 0.1
325 M KCl, 1 mM DTT, 1 mM EDTA, 5 mM ATP, 10 mM $MgCl_2$, 10
326 mM creatine phosphate, 0.1 mg $ml^{-1}$ creatine kinase, 20 mM Tris-
327 MES pH 7.4) and 5 µM of labelled $^3$H-genistein (American
328 Radiolabeled Chemicals, Saint Louis, USA; 1850 Bq $filter^{-1}$). Only
329 for the kinetic experiments, the $^3$H-genistein concentration ranged

330 from 5 μM up to 100 μM (5, 7, 10, 15, 33, 50 and 100 μM $^{3}$H-
331 genistein) and the incubation time was 30 s. The kinetic parameters
332 of $^{3}$H-genistein uptake were calculated by subtracting uptake rates
333 recorded in the empty-vector vesicles. The kinetic parameters of $^{3}$H-
334 genistein uptake were calculated between 7-100 μM by subtracting
335 uptake rates recorded in the empty-vector vesicles using the Hanes–
336 Woolf plot.
337 To test the dependence of genistein transport on a proton gradient,
338 25 mM $NH_4Cl$ was included in the transport buffer assay and the
339 incubation time ranging between 15 and 120 s (15, 30, 60 and 120
340 s). Moreover, the capability of LaMATE2 to mediate the uptake of
341 different flavonoids was tested by UPLC under the same
342 experimental conditions reported above (5 μM of flavonoid:
343 genistein, genistin, hydroxygenistein, biochanin A, daidzein, or
344 kaempferol; the incubation time was 30 s). The mixture was loaded
345 on a pre-wetted filter and removed by suction at the end of
346 incubation time. The membranes were rapidly washed twice with 2
347 ml of ice-cold transport buffer.
348 The radioactive measurements were determined with a beta-counter
349 (Tri-Carb 1900CA, Packard, Downers Grove, USA). As standards,
350 solutions with known amounts of $^{3}$H-genistein were used. Vesicle
351 protein content was quantified with BioRad Protein Assay Dye
352 Reagent (BioRad, Hercules, CA, USA), and the data are shown as
353 pmol $^{3}$H-genistein $\mu g^{-1}$ protein. Data are shown as net pmol $^{3}$H-
354 genistein $\mu g^{-1}$ protein after removing background, i.e. unspecific
355 adsorption of genistein onto empty-vector yeast membrane. Three
356 independent transformations were performed for each sample.
357
358 **LaMATE2 subcellular localization in *Arabidopsis thaliana***
359 **protoplasts**

360 For transient expression of *LaMATE2*$_{ORF}$ in Arabidopsis protoplasts,
361 the plasmid harboring the sequence for the *Green Fluorescent*
362 *Protein* (*GFP*) was fused at the C-terminus of *LaMATE2*$_{ORF}$ inside
363 the pUC18-Sp-GFP6 vector (Komarova et al., 2008) using *NheI* and
364 *SphI* restriction sites via PCR amplification. A plasmid harboring
365 the sequence for *mCherry-fluorescent protein* was fused with
366 *AtPIP2a*, a gene coding for an aquaporin used as a plasma
367 membrane marker (Nelson et al., 2007). Arabidopsis protoplasts
368 were co-transformed with both constructs, *LaMATE2*$_{ORF}$-*GFP* and
369 *AtPIP2a-mCherry*, using the polyethylene glycol method (Jin et al.,
370 2001). Protoplasts were examined with a TCS SP5 confocal
371 microscope (Leica Microsystems, Wetzlar, Germany), excited with
372 an argon laser at 458 nm for GFP and 540–552 nm for mCherry (for
373 GFP: excitation BP458, beamsplitter FT500, emission BP 492-511
374 nm; for mCherry: excitation BP 540–552, beamsplitter FT560,
375 emission BP 575–640).
376
377 **RNAi-based silencing of *LaMATE2* gene in white lupin roots.**
378 *LaMATE2* silencing was adapted from Uhde-Stone and coworkers
379 (2005) using binary transformation vectors, pRNAi and pRedRoot
380 (Limpens et al., 2004). The target region (350 bp long, covering the
381 5' end of *LaMATE2*$_{ORF}$) was first amplified with PCR, and
382 subsequently cloned into pRNAi vector between the restriction sites
383 *NcoI–SwaI* and *BamHI–SpeI*. The cloned sequence (*LaMATE2*
384 *RNAi*) was regulated by a double CaMV35s promoter and OCS-3'
385 terminator. Using the *KpnI–PacI* restriction sites, the *LaMATE2*
386 *RNAi* cassette from the previously produced in pRNAi vector was
387 transfered into the pRedRoot binary vector (pRedRoot::*LaMATE2*
388 *RNAi*).
389
390 **Phylogenetic and Statistical Analyses**

391 Phylogenetic analyses were conducted using MEGA software,
392 version 6 (Tamura et al., 2013). The tree was constructed by aligning
393 the protein sequences by Clustal-W and the evolutionary history was
394 inferred using the Neighbor-Joining method. The percentage of
395 replicate trees in which the associated taxa clustered together in the
396 bootstrap test (1000 replicates) are shown in Fig. **S1** next to the
397 branches. The tree is drawn to scale, with branch lengths in the same
398 units as those of the evolutionary distances used to infer the
399 phylogenetic tree. The evolutionary distances were computed using
400 the Poisson correction method and are in the units of the number of
401 amino acid substitutions per site.
402 The topology prediction of LaMATE2 was performed by using the
403 PROTTER program (Omasits et al., 2014), while the alignment of
404 LaMATE2 protein sequence with orthologous MATE-protein
405 sequences was generated by Clustal-WS using Jalview software
406 version 2 (Waterhouse et al., 2009).
407 Statistical significance was determined by one-way analysis of
408 variances (ANOVA) using Holm–Sidak test, $P < 0.05$ or 0.01.
409 Statistical analyses were calculated using SigmaPlot (Systat
410 Software Inc., San Jose, CA, USA).
411
412
413 **RESULTS AND DISCUSSION**
414 **Release of flavonoids and expression of *LaMATE2***
415 Former work from our laboratories showed that flavonoids are
416 released mainly from the so-called juvenile, and immature (young
417 states) cluster roots and that genistein and its derivative exudation
418 was induced by phosphate (P) deficiency (Weisskopf et al., 2006).
419 Furthermore, in 2001, we published research on genes differentially
420 expressed amongst different stages of cluster roots in P-deficient
421 white lupin (Massonneau et al., 2001). Within these genes, we

422 identified two LaMATE-type transporters, *LaMATE1* was
423 predominantly expressed in mature (Uhde-Stone et al., 2005), citrate
424 excreting cluster roots, while the second (*LaMATE2*) was
425 predominantly present in juvenile cluster roots.
426 To identify a flavonoid exporter possibly playing an important role
427 in the establishment of nodules in *Fabaceae* plants, we looked first
428 whether a link between the expression of *LaMATE2* and release of
429 flavonoids exists. Under P-deficiency, the *LaMATE2* was
430 predominantly expressed in the root apex and in the juvenile stage
431 of cluster roots (Figure 1a). Nitrogen (N) deficiency, on the other
432 hand, induced *LaMATE2* expression mainly in apex and nodule
433 (Figure 2a). Analyses of the root exudates of white lupin revealed
434 that genistein release was strongly induced by P deficiency,
435 particularly in young cluster root tissues (Figure 1b), confirming
436 previous results (Weisskopf et al., 2006). In order to see whether a
437 similar behavior could be observed under N deficiency, plants were
438 grown under N-deficient condition. In this case, cluster root
439 formation was not induced. Hence, we compared the whole roots of
440 plants grown in the presence or absence of N. Nevertheless, we
441 could observe that under N deficiency, genistein release was also
442 increased significantly after 1 and even more pronounced after 2
443 weeks (Figure 2b).
444
445 **Characterization of LaMATE2**
446 As already shown for other MATE transporters, LaMATE2 contains
447 12-transmembrane helical domains (Figure S2) (He et al., 2010).
448 Indeed, LaMATE2 exhibits a good homology to other plant MATE
449 transporters (Figure 3, S2), including the functionally characterized
450 vacuolar flavonoid transporters MtMATE1, MtMATE2 and
451 AtTT12 (Marinova et al., 2007; Zhao and Dixon, 2010; Zhao et al.,
452 2011). Up to date, only few MATE transporters have been

453 characterized in roots and most of them mediate either the efflux of
454 citrate, such as AtFRD3, HvAACT1, SbMATE1 (Durrett et al.,
455 2007; Furukawa et al., 2007; Magalhaes et al., 2007) or act as
456 vacuolar flavonoid transporters in *Arabidopsis*, *Medicago* or
457 grapevine (for a review see Zhao and Dixon (2010) and Zhao
458 (2015)). Interestingly all citrate transporters contain a large
459 cytosolic loop. In white lupin roots and in agreement with our
460 previous results (Massonneau et al., 2001), the expression of another
461 MATE transporter, LaMATE1, a homolog of the citrate transporter
462 AtFRD3, is highest at the mature stage where a burst of citrate
463 exudation occurs (Uhde-Stone et al., 2005; Wang et al., 2014). Also,
464 this transporter contains a large cytosolic loop.
465 At the amino acid level, LaMATE2 exhibits a high similarity to a
466 cluster of MATE proteins, which includes a heterogeneous group of
467 transporters (different substrates, subcellular localization and
468 physiological role). Among the characterized members of this
469 cluster, NtJAT1 and AtDTX1 are the closest homologs of
470 LaMATE2, 55 and 50% of identities, respectively (Figure 3). Both
471 are localized at the plasma membrane (PM) of root cells and
472 function as efflux carriers for plant-derived alkaloids and other toxic
473 compounds (Li et al., 2002; Morita et al., 2009).
474 Several ABC transporters and MATE proteins mediating the export
475 of compounds into the soil have been described (Weston et al., 2012;
476 Baetz and Martinoia, 2014). However, none of them was shown so
477 far to be responsible for the root release of flavonoids and
478 isoflavonoids. Our data showing a connection between flavonoid
479 exudation and *LaMATE2* expression together with the fact that
480 LaMATE2 fused with GFP co-localizes with the PM marker
481 AtPIP2a-mCherry (Figure 4) prompted us to investigate whether
482 LaMATE2 acts as a flavonoid transporter.
483

484 **LaMATE2 silencing reduces genistein release, P mobilization**
485 **and nodule number**
486 Genistein is one of the major released isoflavonoids of *Fabaceae*
487 inducing *NOD* genes in *Rhizobium* bacteria, attracting them and
488 inducing nodule formation (Zhang and Smith, 1995; Lang et al.,
489 2008; Liu and Murray, 2016). Therefore, to assess whether the
490 LaMATE2 might affect genistein release and nodule formation, we
491 have used RNA-dependent gene silencing (*LaMATE2*-RNAi) in
492 roots of white lupin plants. The effectiveness of the silencing was
493 confirmed by a significant reduction (approximatively -80 and 65 %
494 of *LaMATE2* expression in *LaMATE2*-RNAi transformants grown
495 in N and P deficiency, respectively (Figure 5a, g). Analysis of these
496 roots revealed that the release of genistein was strongly reduced in
497 these transformants (Figure 5b, h) and concomitantly isoflavonoids,
498 the uppermost as glycosides, were accumulating in the cell content
499 of silenced roots, which can be regarded as a direct consequence of
500 the reduced genistein exudation (Figure 5d-f). To investigate
501 whether the impaired genistein exudation influences nodulation, we
502 used the *LaMATE2*-RNAi plants to compare the nodule number of
503 silenced and control plants. Our results highlight the importance of
504 LaMATE2-dependent isoflavonoid release in the early step of
505 nodulation, since *LaMATE2* silencing leads to a highly significant
506 reduction (a. -80 %) of nodules in *LaMATE2*-RNAi compared to
507 empty-vector transformed roots (Figure 5c, 6b, S4). Interestingly
508 exogenous application of genistein onto the LaMATE2-RNAi roots
509 partially restored the nodulation efficiency (Figure 6 a, b).
510 Similarly, *LaMATE2* expression, genistein release patterns and
511 capability of root exudates to mobilize P were measured under P-
512 deficient conditions in silenced plants (Figure 5g-i). Cluster roots of
513 *LaMATE2*-RNAi transformants grown under P deficiency released
514 85% less genistein along with the lower level of *LaMATE2*

515 expression (a. -60%). The SPE-purified exudates from those roots
516 also exhibited a limited (a. -66%) mobilization capability from a
517 poorly soluble P source (vivianite). These results suggest that
518 LaMATE2 is the major if not the sole genistein exporter from roots
519 of white lupin plants and in P-deficient condition it contributes to
520 the P solubilization process.
521 The results showing that genistein export is dependent on the
522 presence of LaMATE2 indicates that within the root this transporter
523 is at least partially localized in the cortex. Attempts in our laboratory
524 to get a more detailed picture on its localization, either using in-situ
525 hybridization or a GUS-promoter construct unfortunately failed.
526 However, it should be mentioned that interestingly, excretion of
527 strigolactones into the soil was independent, whether the transporter
528 was localized specifically in hypodermal passage cells as in Petunia
529 or in the whole cortex as in Medicago (Kretzschmar et al., 2012;
530 Banasiak et al., 2020).
531
532 **Transport of phenolics by LaMATE2.**
533 To demonstrate that the reduced genistein release of LaMATE2
534 silenced plants depends directly on the activity of LaMATE2, we
535 expressed it heterologously in *Saccharomyces cerevisiae* and
536 performed transport assays using isolated membrane vesicles
537 (Figure 7). Indeed, using this system, we could observe that
538 LaMATE2 mediates an efficient transport of genistein which was
539 characterized by a saturable kinetic exhibiting an apparent Km of
540 16.2 µM (Figure 7b). This Km is in the same order of magnitude as
541 determined for the vacuolar flavonoid transporters characterized so
542 far (e.g. AtTT12 and MtMATE1: Km of 50 and 36 µM for
543 epicatechin 3′-O-glucoside, respectively; MtMATE2: Km of 88 µM
544 for cyanidin 3-O-glucoside) (Zhao and Dixon, 2010; Zhao et al.,
545 2011). In plasmalemma vesicles isolated from soybean roots,

546 genistein transport exhibited a Km of 160 μM and was strongly
547 dependent on the presence of ATP (Sugiyama et al., 2007).
548 Up to date, certain MATEs have been shown to exhibit a broad range
549 of substrate specificity (Takanashi et al., 2014), while LaMATE2
550 displays a strong specificity for the substrate genistein (Figure 6c).
551 Besides genistein, LaMATE2 was able to transport only daidzein at
552 a low rate, but not other tested flavonoids such as genistin (a
553 glycosylated form of genistein), hydroxygenistein, biochanin A (a
554 methylated form of genistein) or kaempferol. Previous observations
555 in soybean showed that the presence of daidzein in the external
556 media strongly limited genistein transport in plasma membrane
557 vesicles of root cells, indicating a possible competition between
558 those molecules (Sugiyama et al., 2007).
559 A feature of MATE proteins is to couple the substrate transport to
560 an electrochemical gradient, working as $H^+$ or $Na^+$/substrate
561 antiporters (He et al., 2010; Lu et al., 2013; Tanaka et al., 2013). Our
562 results showed that ATP-dependent $^3$H-genistein accumulation in
563 vesicles deriving from *LaMATE2*$_{ORF}$-expressing yeast was strongly
564 reduced in presence of ammonium chloride, which dissipates the
565 transmembrane proton gradient (Marinova et al., 2007; Zhao and
566 Dixon, 2010) (Figure 7a), indicating that LaMATE2 acts as a
567 substrate-proton co-transporter, similarly to AtTT12 (Marinova et
568 al., 2007), AtDTX1 (Li et al., 2002) and NtJAT1 (Morita et al.,
569 2009).
570
571 **Conclusions**
572 In this work the long-sought-after isoflavonoid plasma membrane
573 exporter required to attract symbiotic bacteria for N fixation has
574 been identified. Different *leguminous* plants release different sets of
575 isoflavonoids to induce nodulation (Liu and Murray, 2016).
576 Released genistein has been indicated in faba bean and soybean as

577 *rhizobia* attractant (Zhang and Smith, 1995; Li et al., 2016). Since
578 *Medicago truncatula* and soybean both encode one MATE protein
579 that exhibits high homology to LaMATE2, it is tempting to
580 speculate that these homologues could also act as isoflavonoid
581 exporters, possibly showing slightly different substrate preferences
582 according to the isoflavonoid produced by the plant to initiate the
583 symbiosis. However, it cannot be excluded that in addition to
584 MATE-type transporters and some ABC transporters are also
585 involved in isoflavonoid release. Since isoflavonoids can also
586 release Pi from minerals (Cesco et al., 2010) and organic complexes
587 these transporters may play a dual role in N and P supply.
588
589 During the last years, we learned a lot about the signaling pathways
590 and the effectors involved in establishing the legume-*rhizobia*
591 symbiosis. Surprisingly molecular identity of membrane
592 transporters responsible for the release of phenolic compounds
593 initiating interactions was not known. With the identification of
594 LaMATE2 we succeeded to identify the very initial step leading to
595 this symbiosis. Since there is a huge interest to transfer this complex
596 mechanism to other crop plants to grow them in the absence of
597 artificial N-sources we do believe that it is a valuable piece of the
598 puzzle to consider in such an ambitious project.
599
600 **ACKNOWLEDGEMENTS**
601 Research was supported by grants from Italian Ministry of
602 University and Research-MIUR (FIRB-Programme Futuro in
603 Ricerca, RBFR08L2ZT and RBFR127WJ9), from funds of the
604 Zurich University; and statutory funds from the Polish Ministry of
605 Science and Higher Education. **Competing interests:** Authors
606 declare no competing interests; and **Data and materials**
607 **availability:** Sequence data from this article can be found in the

608 EMBL/GenBank data libraries under accession number KY464927,
609 LaMATE2 of *Lupinus albus*.
610
611 **AUTHOR CONTRIBUTION**
612 NT, EM, RP, SC, MJ: designed and oversaw the research; WB,
613 LZ, SG, RBF, SV, FV, TM, BB, NT: performed experiments and
614 analyzed data; NT, EM, RP, MJ: wrote the paper
615

616 **REFERENCES**

617


618 Baetz, U., and Martinoia, E. (2014). Root exudates: the hidden part
619 of plant defense. *Trends in Plant Science* 19**,** 90-98.
620 Banasiak, J., Borghi, L., Stec, N., Martinoia, E., and Jasiński, M.
621 (2020). The Full-Size ABCG Transporter of *Medicago*
622 *truncatula* Is Involved in Strigolactone Secretion, Affecting
623 Arbuscular Mycorrhiza. 11.
624 Biala, W., Banasiak, J., Jarzyniak, K., Pawela, A., and Jasinski, M.
625 (2017). Medicago truncatula ABCG10 is a transporter of 4-
626 coumarate and liquiritigenin in the medicarpin biosynthetic
627 pathway. *Journal of experimental botany* 68**,** 3231-3241.
628 Burke, D., Dawson, D., and Stearns, T. (2000). Methods in yeast
629 genetics: a Cold Spring Harbor Laboratory course manual,
630 2000 ed. *Cold Spring Harbor Press: Plainview, NY* 17**,**
631 205.
632 Cesco, S., Neumann, G., Tomasi, N., Pinton, R., and Weisskopf, L.
633 (2010). Release of plant-borne flavonoids into the
634 rhizosphere and their role in plant nutrition. *Plant and Soil*
635 329**,** 1-25.
636 Durrett, T.P., Gassmann, W., and Rogers, E.E. (2007). The FRD3-
637 Mediated Efflux of Citrate into the Root Vasculature Is
638 Necessary for Efficient Iron Translocation. *Plant*
639 *Physiology* 144**,** 197-205.
640 Furukawa, J., Yamaji, N., Wang, H., Mitani, N., Murata, Y., Sato,
641 K., Katsuhara, M., Takeda, K., and Ma, J.F. (2007). An
642 Aluminum-Activated Citrate Transporter in Barley. *Plant*
643 *and Cell Physiology* 48**,** 1081-1091.
644 Gietz, R.D., and Woods, R.A. (2002). Transformation of yeast by
645 lithium acetate/single-stranded carrier DNA/polyethylene
646 glycol method. *Methods in enzymology* 350**,** 87-96.

He, X., Szewczyk, P., Karyakin, A., Evin, M., Hong, W.-X., Zhang, Q., and Chang, G. (2010). Structure of a cation-bound multidrug and toxic compound extrusion transporter. *Nature* 467**,** 991.

Hufnagel, B., Marques, A., Soriano, A., Marquès, L., Divol, F., Doumas, P., Sallet, E., Mancinotti, D., Carrere, S., Marande, W., Arribat, S., Keller, J., Huneau, C., Blein, T., Aimé, D., Laguerre, M., Taylor, J., Schubert, V., Nelson, M., Geu-Flores, F., Crespi, M., Gallardo, K., Delaux, P.-M., Salse, J., Bergès, H., Guyot, R., Gouzy, J., and Péret, B. (2020). High-quality genome sequence of white lupin provides insight into soil exploration and seed quality. *Nature Communications* 11**,** 492.

Jiang, Y., Wang, W., Xie, Q., Liu, N., Liu, L., Wang, D., Zhang, X., Yang, C., Chen, X., Tang, D., and Wang, E. (2017). Plants transfer lipids to sustain colonization by mutualistic mycorrhizal and parasitic fungi. *Science* 356**,** 1172-1175.

Jin, J.B., Kim, Y.A., Kim, S.J., Lee, S.H., Kim, D.H., Cheong, G.W., and Hwang, I. (2001). A new dynamin-like protein, ADL6, is involved in trafficking from the *trans*-Golgi network to the central vacuole in Arabidopsis. *The Plant cell* 13**,** 1511-1526.

Klein, M., Mamnun, Y.M., Eggmann, T., Schüller, C., Wolfger, H., Martinoia, E., and Kuchler, K. (2002). The ATP-binding cassette (ABC) transporter Bpt1p mediates vacuolar sequestration of glutathione conjugates in yeast. *FEBS letters* 520**,** 63-67.

Komarova, N.Y., Thor, K., Gubler, A., Meier, S., Dietrich, D., Weichert, A., Suter Grotemeyer, M., Tegeder, M., and Rentsch, D. (2008). AtPTR1 and AtPTR5 Transport Dipeptides in Planta. *Plant Physiology* 148**,** 856-869.

Koressaar, T., and Remm, M. (2007). Enhancements and modifications of primer design program Primer3. *Bioinformatics* 23**,** 1289-1291.

Kretzschmar, T., Kohlen, W., Sasse, J., Borghi, L., Schlegel, M., Bachelier, J.B., Reinhardt, D., Bours, R., Bouwmeester, H.J., and Martinoia, E. (2012). A petunia ABC protein controls strigolactone-dependent symbiotic signalling and branching. *Nature* 483**,** 341-344.

Lambers, H., Martinoia, E., and Renton, M. (2015). Plant adaptations to severely phosphorus-impoverished soils. *Current Opinion in Plant Biology* 25**,** 23-31.

Lang, K., Lindemann, A., Hauser, F., and Göttfert, M. (2008). The genistein stimulon of *Bradyrhizobium japonicum*. *Molecular Genetics and Genomics* 279**,** 203-211.

692 Li, B., Li, Y.-Y., Wu, H.-M., Zhang, F.-F., Li, C.-J., Li, X.-X.,
693 Lambers, H., and Li, L. (2016). Root exudates drive
694 interspecific facilitation by enhancing nodulation and $N_2$
695 fixation. *Proceedings of the National Academy of Sciences*
696 113**,** 6496-6501.
697 Li, L., He, Z., Pandey, G.K., Tsuchiya, T., and Luan, S. (2002).
698 Functional Cloning and Characterization of a Plant Efflux
699 Carrier for Multidrug and Heavy Metal Detoxification.
700 *Journal of Biological Chemistry* 277**,** 5360-5368.
701 Limpens, E., Ramos, J., Franken, C., Raz, V., Compaan, B.,
702 Franssen, H., Bisseling, T., and Geurts, R. (2004). RNA
703 interference in *Agrobacterium rhizogenes*-transformed
704 roots of *Arabidopsis* and *Medicago truncatula*. *Journal of*
705 *Experimental Botany* 55**,** 983-992.
706 Liu, C.-W., and Murray, J. (2016). The Role of Flavonoids in
707 Nodulation Host-Range Specificity: An Update. *Plants* 5**,**
708 33.
709 Livak, K.J., and Schmittgen, T.D. (2001). Analysis of Relative
710 Gene Expression Data Using Real-Time Quantitative PCR
711 and the $2^{-\Delta\Delta CT}$ Method. *Methods* 25**,** 402-408.
712 Lu, M., Radchenko, M., Symersky, J., Nie, R., and Guo, Y. (2013).
713 Structural insights into $H^+$-coupled multidrug extrusion by
714 a MATE transporter. *Nature Structural & Molecular*
715 *Biology* 20**,** 1310-1317.
716 Luginbuehl, L.H., Menard, G.N., Kurup, S., Van Erp, H.,
717 Radhakrishnan, G.V., Breakspear, A., Oldroyd, G.E.D., and
718 Eastmond, P.J. (2017). Fatty acids in arbuscular
719 mycorrhizal fungi are synthesized by the host plant.
720 *Science* 356**,** 1175-1178.
721 Magalhaes, J.V., Liu, J., Guimaraes, C.T., Lana, U.G.P., Alves,
722 V.M.C., Wang, Y.H., Schaffert, R.E., Hoekenga, O.A.,
723 Pineros, M.A., Shaff, J.E., Klein, P.E., Carneiro, N.P.,
724 Coelho, C.M., Trick, H.N., and Kochian, L.V. (2007). A
725 gene in the multidrug and toxic compound extrusion
726 (MATE) family confers aluminum tolerance in sorghum.
727 *Nature Genetics* 39**,** 1156-1161.
728 Marinova, K., Kleinschmidt, K., Weissenbock, G., and Klein, M.
729 (2007). Flavonoid Biosynthesis in Barley Primary Leaves
730 Requires the Presence of the Vacuole and Controls the
731 Activity of Vacuolar Flavonoid Transport. *Plant*
732 *Physiology* 144**,** 432-444.
733 Martin, F.M., Uroz, S., and Barker, D.G. (2017). Ancestral
734 alliances: Plant mutualistic symbioses with fungi and
735 bacteria. *Science* 356**,** eaad4501.
736 Massonneau, A., Langlade, N., Leon, S., Smutny, J., Vogt, E.,
737 Neumann, G., and Martinoia, E. (2001). Metabolic changes

associated with cluster root development in white lupin (*Lupinus albus* L.): relationship between organic acid excretion, sucrose metabolism and energy status. *Planta* 213**,** 534-542.

Morita, M., Shitan, N., Sawada, K., Van Montagu, M.C.E., Inzé, D., Rischer, H., Goossens, A., Oksman-Caldentey, K.-M., Moriyama, Y., and Yazaki, K. (2009). Vacuolar transport of nicotine is mediated by a multidrug and toxic compound extrusion (MATE) transporter in *Nicotiana tabacum*. *Proceedings of the National Academy of Sciences of the United States of America* 106**,** 2447-2452.

Nelson, B.K., Cai, X., and Nebenführ, A. (2007). A multicolored set of in vivo organelle markers for co-localization studies in *Arabidopsis* and other plants. *The Plant Journal* 51**,** 1126-1136.

Neumann, G., and Martinoia, E. (2002). Cluster roots - an underground adaptation for survival in extreme environments. *Trends in Plant Science* 7**,** 162-167.

Omasits, U., Ahrens, C.H., Müller, S., and Wollscheid, B. (2014). Protter: interactive protein feature visualization and integration with experimental proteomic data. *Bioinformatics* 30**,** 884-886.

Purnell, H.M. (1960). Studies of the family Proteaceae. Anatomy and morphology of the roots of some Victorian species. *Australian Journal of Botany* 8**,** 38-50.

Quandt, H.J., Pühler, A., and Broer, I. (1993). Transgenic root nodules of *Vicia hirsuta:* a fast and efficient system for the study of gene expression in indeterminate-type nodules. *MPMI-Molecular Plant Microbe Interactions* 6**,** 699-706.

Ritz, C., and Spiess, A.N. (2008). qpcR: an R package for sigmoidal model selection in quantitative real-time polymerase chain reaction analysis. *Bioinformatics* 24**,** 1549-1551.

Sauer, N., and Stolz, J. (1994). SUC1 and SUC2: two sucrose transporters from *Arabidopsis thaliana*; expression and characterization in baker's yeast and identification of the histidine-tagged protein. *The Plant Journal* 6**,** 67-77.

Staszków, A., Swarcewicz, B., Banasiak, J., Muth, D., Jasiński, M., and Stobiecki, M. (2011). LC/MS profiling of flavonoid glycoconjugates isolated from hairy roots, suspension root cell cultures and seedling roots of Medicago truncatula. *Metabolomics* 7**,** 604-613.

Stępkowski, T., Żak, M., Moulin, L., Króliczak, J., Golińska, B., Narożna, D., Safronova, V.I., and Mądrzak, C.J. (2011). *Bradyrhizobium canariense* and *Bradyrhizobium japonicum* are the two dominant *rhizobium* species in root

784 nodules of lupin and serradella plants growing in Europe.
785 *Systematic and Applied Microbiology* 34**,** 368-375.
786 Strozycki, P.M., Skąpska, A., Szcześniak, K., Sobieszczuk, E.,
787 Briat, J.-F., and Legocki, A.B. (2003). Differential
788 expression and evolutionary analysis of the three ferritin
789 genes in the legume plant *Lupinus luteus*. *Physiologia*
790 *Plantarum* 118**,** 380-389.
791 Subramanian, S., Stacey, G., and Yu, O. (2006). Endogenous
792 isoflavones are essential for the establishment of symbiosis
793 between soybean and *Bradyrhizobium japonicum*. *The*
794 *Plant Journal* 48**,** 261-273.
795 Sugiyama, A., Shitan, N., and Yazaki, K. (2007). Involvement of a
796 soybean ATP-binding cassette-Type transporter in the
797 secretion of genistein, a signal flavonoid in legume-
798 *Rhizobium* Symbiosis. *Plant Physiology* 144**,** 2000-2008.
799 Takanashi, K., Shitan, N., and Yazaki, K. (2014). The multidrug
800 and toxic compound extrusion (MATE) family in plants.
801 *Plant Biotechnology* 31**,** 417-430.
802 Tamura, K., Stecher, G., Peterson, D., Filipski, A., and Kumar, S.
803 (2013). MEGA6: Molecular Evolutionary Genetics
804 Analysis version 6.0. *Molecular biology and evolution* 30**,**
805 2725-2729.
806 Tanaka, Y., Hipolito, C.J., Maturana, A.D., Ito, K., Kuroda, T.,
807 Higuchi, T., Katoh, T., Kato, H.E., Hattori, M., Kumazaki,
808 K., Tsukazaki, T., Ishitani, R., Suga, H., and Nureki, O.
809 (2013). Structural basis for the drug extrusion mechanism
810 by a MATE multidrug transporter. *Nature* 496**,** 247-251.
811 Tilman, D. (1999). Global environmental impacts of agricultural
812 expansion: The need for sustainable and efficient practices.
813 *Proceedings of the National Academy of Sciences* 96**,** 5995-
814 6000.
815 Tilman, D., Fargione, J., Wolff, B., D'antonio, C., Dobson, A.,
816 Howarth, R., Schindler, D., Schlesinger, W.H., Simberloff,
817 D., and Swackhamer, D. (2001). Forecasting Agriculturally
818 Driven Global Environmental Change. *Science* 292**,** 281-
819 284.
820 Udvardi, M., and Poole, P.S. (2013). Transport and Metabolism in
821 Legume-*Rhizobia* Symbioses. *Annual Review of Plant*
822 *Biology* 64**,** 781-805.
823 Uhde-Stone, C., Liu, J., Zinn, K.E., Allan, D.L., and Vance, C.P.
824 (2005). Transgenic proteoid roots of white lupin: a vehicle
825 for characterizing and silencing root genes involved in
826 adaptation to P stress. *Plant Journal* 44**,** 840-853.
827 Untergasser, A., Cutcutache, I., Koressaar, T., Ye, J., Faircloth,
828 B.C., Remm, M., and Rozen, S.G. (2012). Primer3—new

829 capabilities and interfaces. *Nucleic Acids Research* 40**,**
830 e115.
831 Vance, C.P., Uhde-Stone, C., and Allan, D.L. (2003). Phosphorus
832 acquisition and use: critical adaptations by plants for
833 securing a nonrenewable resource. *New Phytologist* 157**,**
834 423-447.
835 Wang, Z., Straub, D., Yang, H., Kania, A., Shen, J., Ludewig, U.,
836 and Neumann, G. (2014). The regulatory network of
837 cluster-root function and development in phosphate-
838 deficient white lupin (*Lupinus albus*) identified by
839 transcriptome sequencing. *Physiologia Plantarum* 151**,**
840 323-338.
841 Wasson, A.P., Pellerone, F.I., and Mathesius, U. (2006). Silencing
842 the flavonoid pathway in *Medicago truncatula* inhibits root
843 nodule formation and prevents auxin transport regulation
844 by rhizobia. *Plant Cell* 18**,** 1617-1629.
845 Waterhouse, A.M., Procter, J.B., Martin, D.M.A., Clamp, M., and
846 Barton, G.J. (2009). Jalview Version 2—a multiple
847 sequence alignment editor and analysis workbench.
848 *Bioinformatics* 25**,** 1189-1191.
849 Weisskopf, L., Tomasi, N., Santelia, D., Martinoia, E., Langlade,
850 N.B., Tabacchi, R., and Abou-Mansour, E. (2006).
851 Isoflavonoid exudation from white lupin roots is influenced
852 by phosphate supply, root type and cluster-root stage. *New*
853 *Phytologist* 171**,** 657-668.
854 Weston, L.A., Ryan, P.R., and Watt, M. (2012). Mechanisms for
855 cellular transport and release of allelochemicals from plant
856 roots into the rhizosphere. *Journal of Experimental Botany*.
857 Zhang, F., and Smith, D.L. (1995). Preincubation of
858 Bradyrhizobium japonicum with Genistein Accelerates
859 Nodule Development of Soybean at Suboptimal Root Zone
860 Temperatures. *Plant Physiology* 108**,** 961-968.
861 Zhao, J. (2015). Flavonoid transport mechanisms: how to go, and
862 with whom. *Trends in Plant Science* 20**,** 576-585.
863 Zhao, J., and Dixon, R.A. (2010). The 'ins' and 'outs' of flavonoid
864 transport. *Trends in Plant Science* 15**,** 72-80.
865 Zhao, J., Huhman, D., Shadle, G., He, X.-Z., Sumner, L.W., Tang,
866 Y., and Dixon, R.A. (2011). MATE2 Mediates Vacuolar
867 Sequestration of Flavonoid Glycosides and Glycoside
868 Malonates in *Medicago truncatula*. *The Plant Cell* 23**,**
869 1536-1555.

870

871
872
873

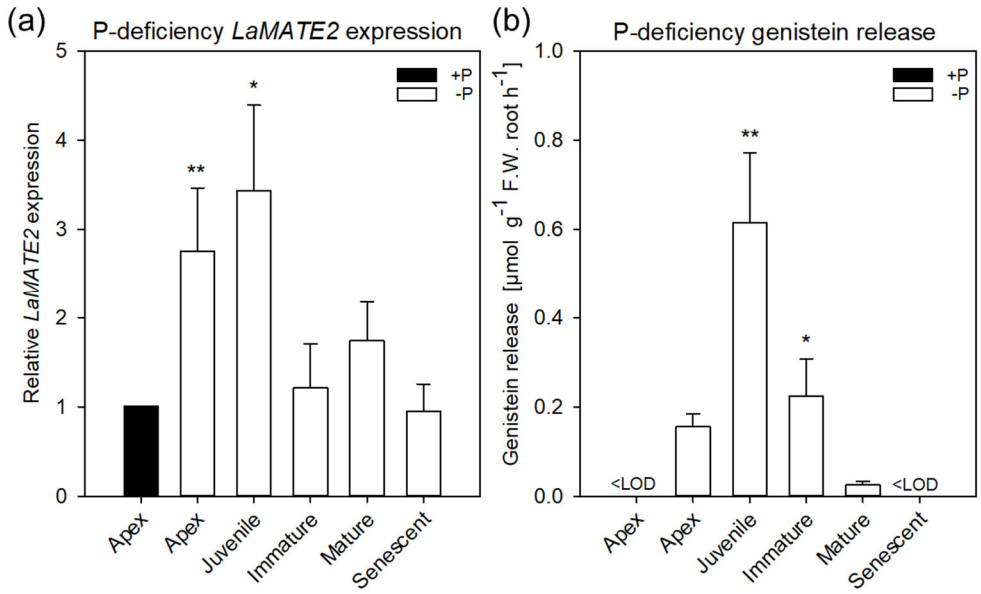


**Figure 1. *LaMATE2* expression level and genistein release in roots of P-deficient white lupin**

*LaMATE2* expression analyses in white lupin grown under control (+N+P, black bars) condition or P deficiency (+N-P, white bars) (**a**). Gene expression was evaluated in control apex (+N+P), P-deficient apex and cluster roots (separated depending on developing stages: Juvenile, Immature, Mature, Senescent cluster-root stages; example of cluster root shown in Figure S1). Expression levels are shown relative to the *LaMATE2* expression level of the root apex under control conditions (+N+P). Release of genistein from different root tissues of 4-week-old P-deficient plants, release from the control apex was below detectable value <LOD (**b**). Data are means +SD (* refer to statistically significant differences among the mean value of the sample *vs* control or -P apex for genistein release, ANOVA Holm–Sidak, N=6, *P <0.05, ** P <0.01).

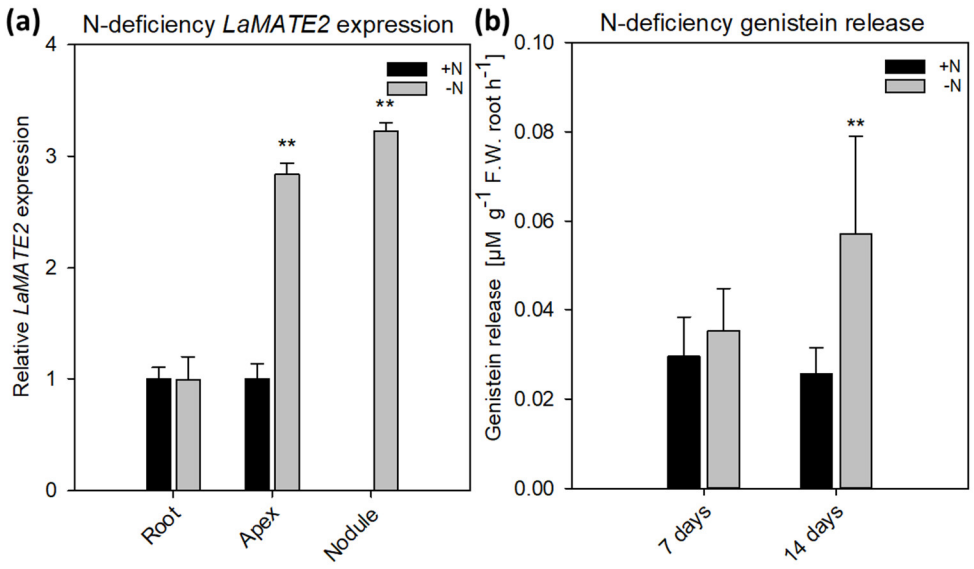


889

890 **Figure 2. *LaMATE2* expression analyses and genistein release in**
891 **roots of N-deficient white lupin**

892 *LaMATE2* expression analyses in white lupin grown under control
893 (+N+P, black bars) condition or N-deficiency (-N+P, dark grey bars)
894 (**a**). Gene expression was evaluated in control and N-deficient
895 (other) root, root apex and nodules. Expression level is shown
896 relative to *LaMATE2* expression in control (+N+P) root. Root
897 release of genistein from white lupin plants grown under 1- or 2-
898 week-old N-sufficient and -deficient condition (**b**). Genistein release
899 in 7 and 14 days of N deficiency (-N+P) or sufficiency (+N+P) .
900 Data are means +SD (* refers to statistically significant differences
901 among the mean value of the sample *vs* control, ANOVA Holm–
902 Sidak, N=6, * P <0.05, ** P <0.01).

903

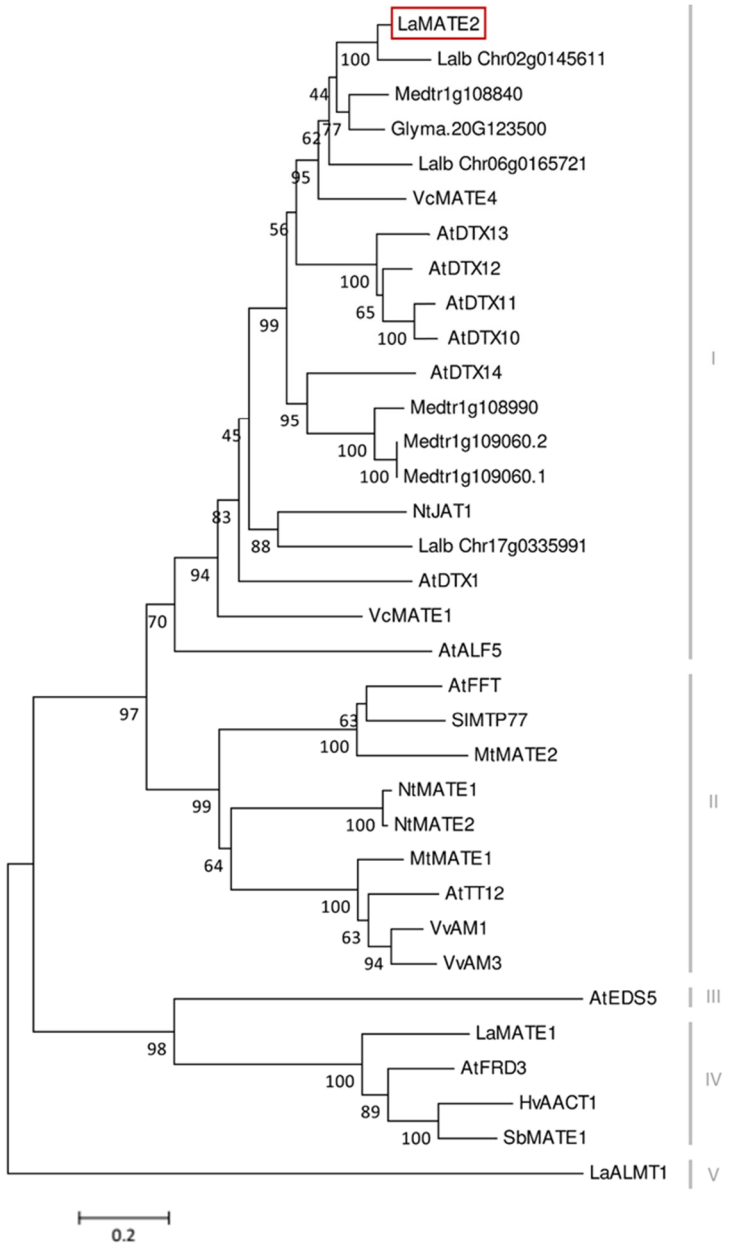


904

905 **Figure 3. Phylogenetic tree of MATE transporters**

906 A phylogenetic analysis was performed using the LaMATE2 amino
907 acid sequences of *Lupinus albus* (LaMATE1, LaMATE2,
908 Lalb_Chr17g0335991, Lalb_Chr06g0165721,
909 Lalb_Chr02g0145611, LaALMT1); AtFRD3 AtEDS5, AtTT12,
910 AtDTX1,10,11,12,13,14, AtALF5 and AtFFT of *Arabidopsis*
911 *thaliana*; Glyma.10G267700 of *Glycine max*; HvAACT1 of
912 *Hordeum vulgare*; MtMATE1, MtMATE2, Medtr1g108840,
913 Medtr1g108990, Medtr1g109060.2, Medtr1g109060.1 of *Medicago*
914 *truncatula*; NtJAT1, NtMATE1 and NtMATE2 of *Nicotiana*

915 *tabacum*; SlMTP77 of *Solanum lycopersicum*; SbMATE1 of
916 *Sorghum bicolor*; VvAM1 and VvAM3 of *Vitis vinifera*; VcMATE1
917 and VcMATE4 of *Vaccinium corymbosum*. The tree was
918 constructed by aligning the protein sequences by Clustal-W and the
919 evolutionary history was inferred using the Neighbour-Joining
920 method. The percentage of replicate trees in which the associated
921 taxa clustered together in the bootstrap test (1000 replicates) are
922 shown next to the branches. The tree is drawn to scale, with branch
923 lengths in the same units as those of the evolutionary distances used
924 to infer the phylogenetic tree. The evolutionary distances were
925 computed using the Poisson correction method and are in the units
926 of the number of amino acid substitutions per site.

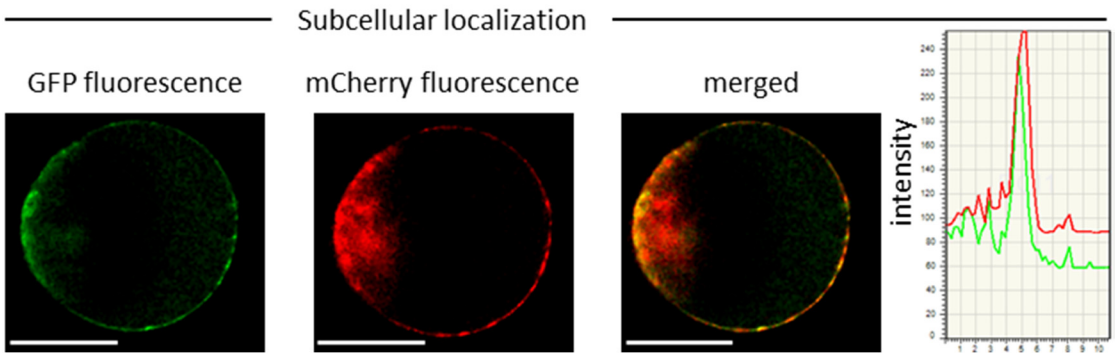


927

928 **Figure 4. Subcellular localization of LaMATE2**

929 Co-localization of LaMATE2 fused with green fluorescent protein
930 (GFP) and mCherry-labeled plasma membrane marker AtPIP2A in
931 an Arabidopsis mesophyll protoplast. White scale bars = 20 µm.
932 Fluorescence intensity over distance plot of LaMATE2-GFP (green)
933 and AtPIP2a-mCherry (red).

934

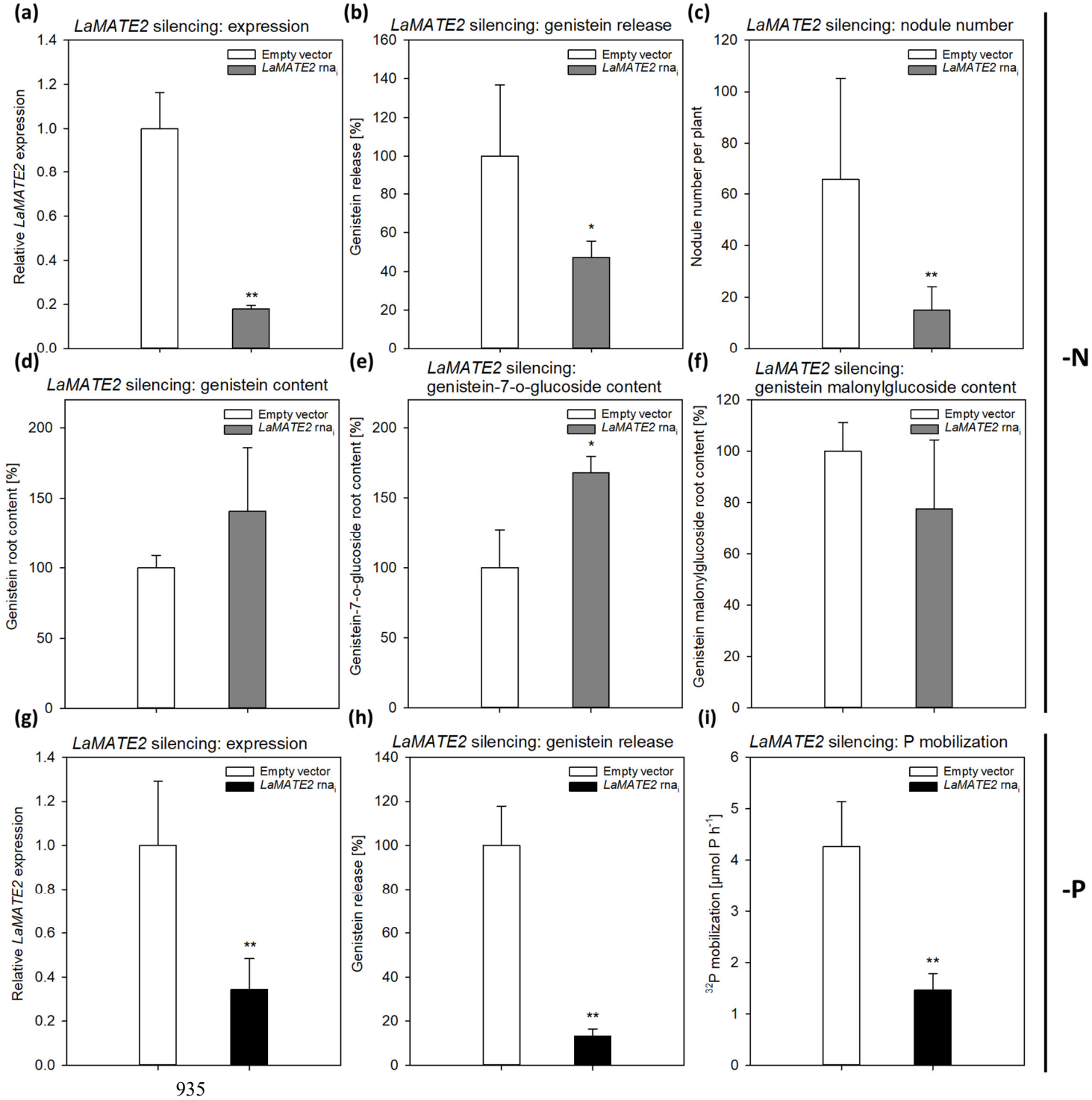


935

936 **Figure 5. Effect of *LaMATE2* silencing in N and P deficient roots**

937 Alteration of *LaMATE2* expression, flavonoid content and release,
938 nodule number or P mobilization due to *LaMATE2* silencing in N
939 (**a-f**) or P (**g-i**) deficiency. *LaMATE2* relative expression (**a, g**),

940 genistein release (**b, h**), number of nodules per plant (pictures shown
941 in Figure S4) (**c**), cell content: genistein (**d**), genistein 7-O-glucoside
942 (**e**), genistein malonylglucoside (**f**), P mobilization from a poorly
943 soluble P source (**i**). The analyses were performed on roots of N- or
944 P-deficient lupin plants independently transformed with either
945 pRedRoot::*LaMATE2* RNAi (*LaMATE2* RNAi) or empty-vector
946 pRedRoot (Empty vector).
947 All data are expressed relative to Empty-vector-transformed roots,
948 with the exceptions of the number of nodule per plants and P
949 mobilization (µmol P $h^{-1}$). Data are means+SD (* refers to
950 statistically significant differences among the mean value of RNAi
951 and Empty vector, ANOVA Holm–Sidak, N=6-21, *P <0.05; ** for
952 P<0.01).

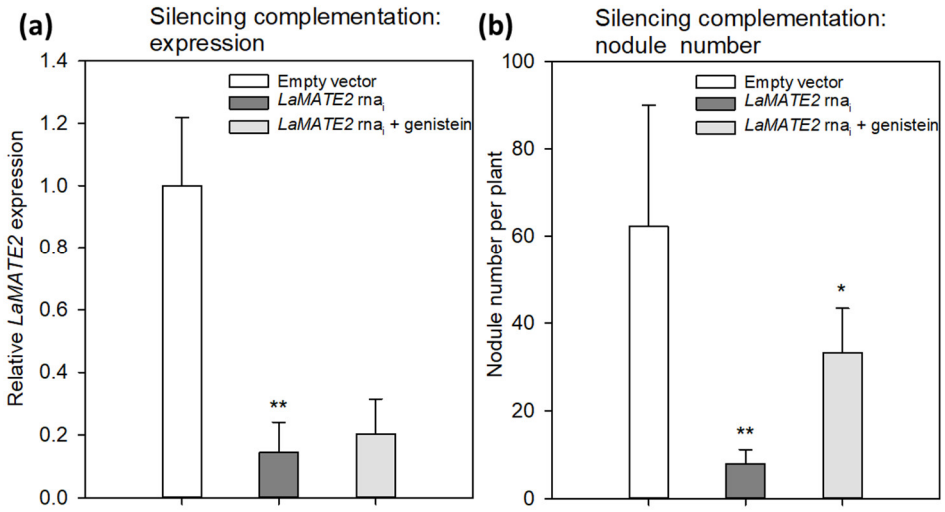


**Figure 6. Effect of exogenous genistein on *LaMATE2* expression and nodule numbers**

*LaMATE2* relative expression (**a**) and number of nodules per plant (**b**) in roots of N-deficient lupin plants independently transformed with either pRedRoot::*LaMATE2* RNAi (*LaMATE2* RNAi) or empty-vector pRedRoot (Empty vector) or RNAi roots treated with 1 µM genistein (*LaMATE2* RNAi + genistein).
Expression data are shown relative to *LaMATE2* expression level in empty vector-transformed roots. Data are means+SD (* refers to statistically significant differences among the mean value of RNAi and EV or RNAi+G values, ANOVA Holm–Sidak, N=6, *P <0.05; ** for P<0.01).

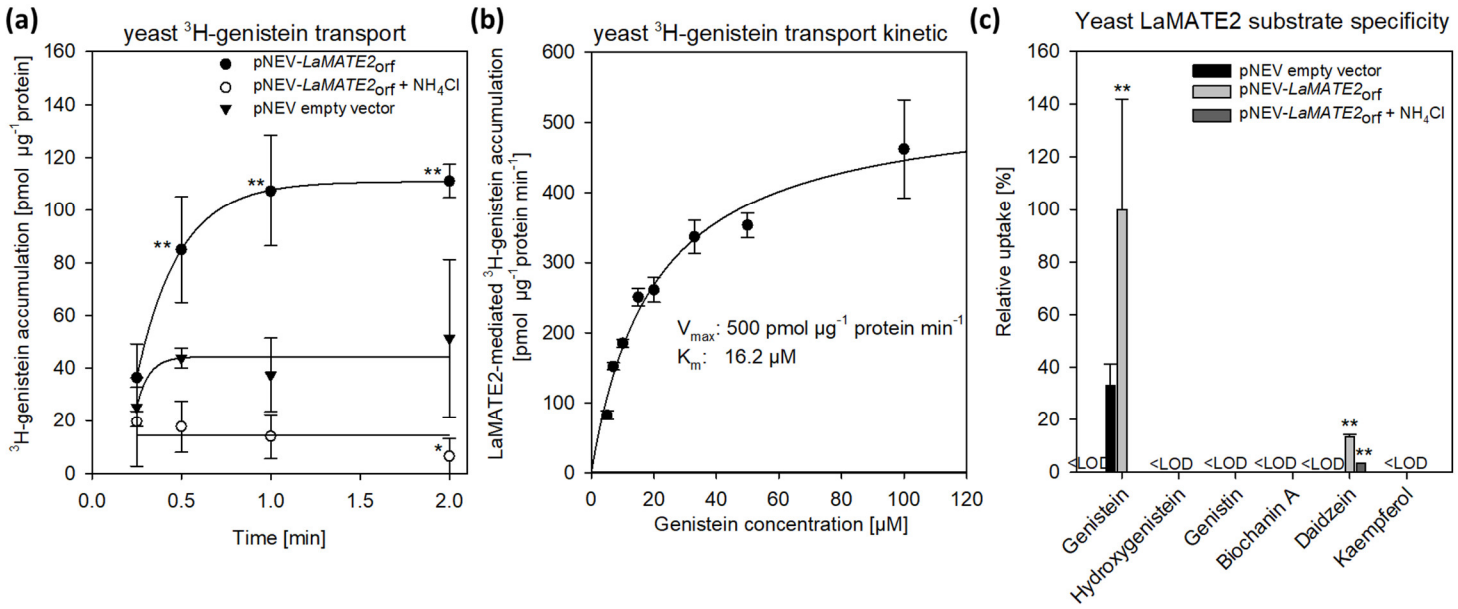


**Figure 7. Transport of phenylpropanoid compounds mediated by LaMATE2**

LaMATE2-mediated transport rate of phenylpropanoids in yeast microsomal membrane vesicles. (**A**) Time-dependent accumulation of $^{3}$H-genistein in yeast microsomal membrane vesicles. Membrane vesicles were isolated from yeast transformed with the empty vector (pNEV empty vector) or transformed with pNEV-*LaMATE2*$_{ORF}$. The yeast vesicles were incubated up to 120 s in presence of 5 µM $^{3}$H-genistein: To determine the effect of the pH gradient, 25 mM $NH_4Cl$ was added in an assay solution (pNEV-*LaMATE2*$_{ORF}$ + $NH_4Cl$), as uncoupler of the proton gradient. (**B**) Concentration-dependent transport of $^{3}$H-genistein by LaMATE2 in yeast vesicles. Vesicles were incubated for 30 s in the assay solution containing $^{3}$H-genistein at different concentrations (from 5 to 100 µM). The kinetic parameters of $^{3}$H-genistein uptake were calculated by subtracting uptake rates recorded in the empty-vector vesicles using the Hanes–Woolf plot. (**C**) Substrate specificity of LaMATE2 transporter was evaluated in presence of genistein, hydroxygenistein, genistin (glycosylated genistein), biochanin A (methylgenistein), daidzein or kaempferol (5 µM, 30 s). All data are expressed relative to pNEV-*LaMATE2*$_{ORF}$-transformed yeast. Data are means±SD of three independent experiments (*refers to statistically significant differences among the mean value in comparison to empty vector sample within each time point; capital letters refer to statistically significant differences among the mean value, ANOVA Holm–Sidak, N=6, *P <0.05, **P <0.01, <LOD: below detectable value).

995

996 **Supplementary materials**

997

998

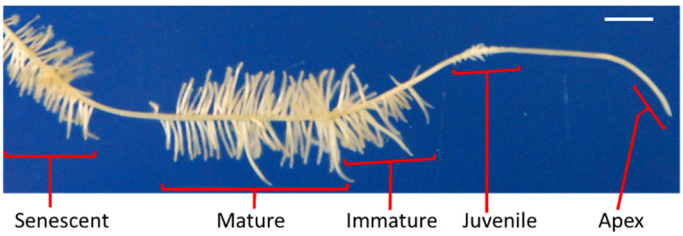


999

1000

1001 **Figure S1. Cluster roots of P-deficient white lupin**

1002

1003 Picture of a lateral root of a 4-week-old white lupin grown under P-
1004 deficient condition (+N-P). The different developing stages:
1005 Juvenile, Immature, Mature, Senescent cluster-root stage and Apex
1006 tissue [10 mm from the root tips] are highlighted and named. White
1007 scale bar = 10 mm.

1008

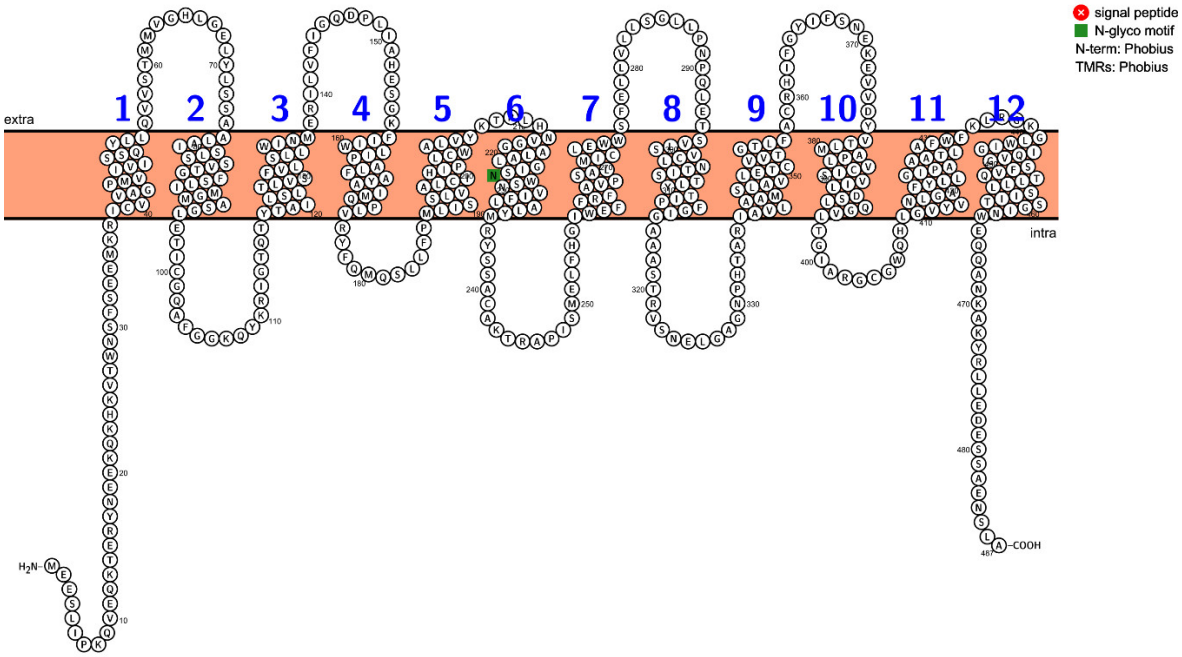


**Figure S2. Predicted membrane topology for LaMATE2 from white lupin**

The model was obtained by using the PROTTER program (Omasits *et al.,* 2014).

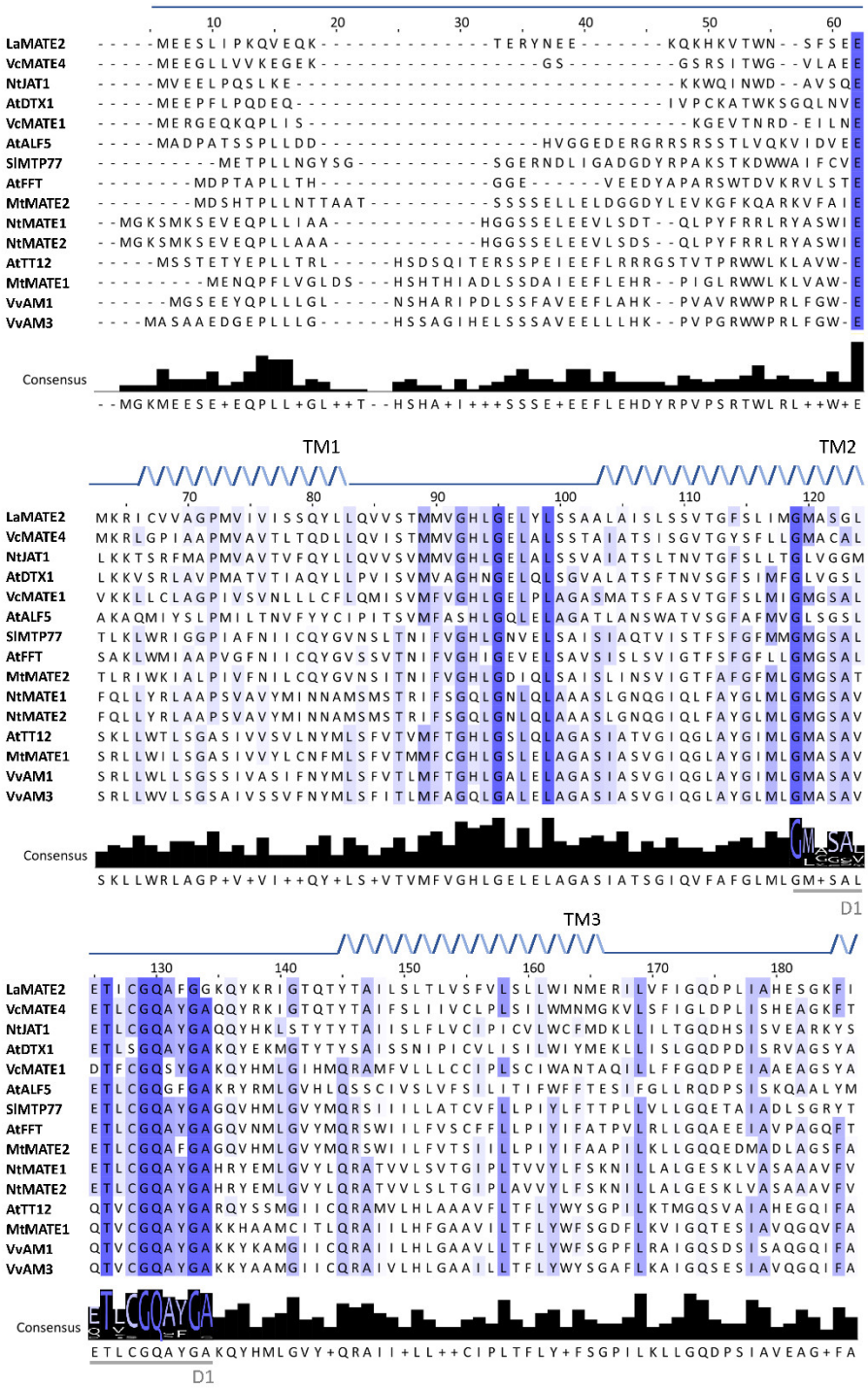
LaMATE2
VcMATE4
NtJAT1
AtDTX1
VcMATE1
AtALF5
SlMTP77
AtFFT
MtMATE2
NtMATE1
NtMATE2
AtTT12
MtMATE1
VvAM1
VvAM3
Consensus
TM1
TM2
TM3
D1

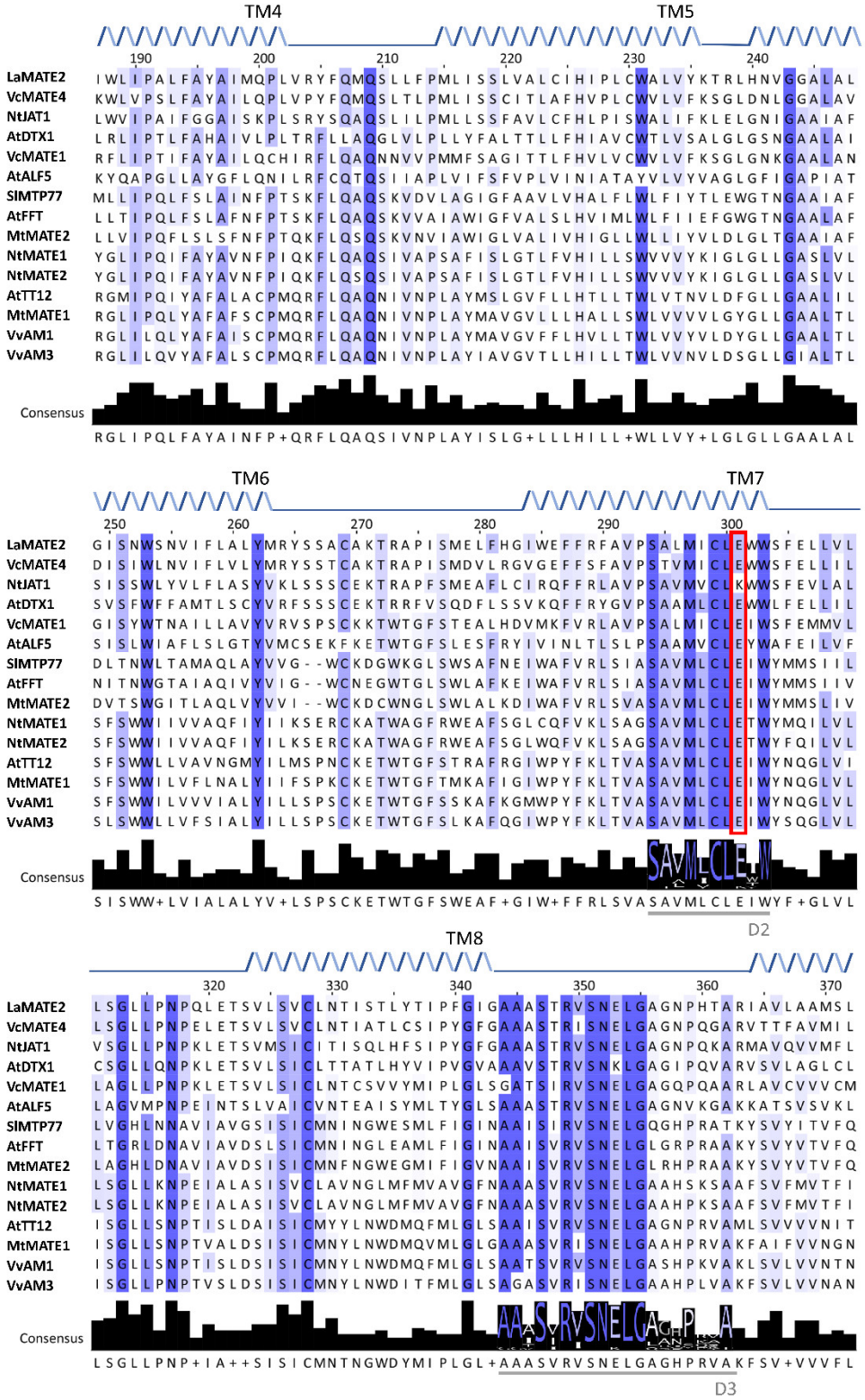
TM4
TM5
190
200
210
220
230
240
LaMATE2
VcMATE4
NtJAT1
AtDTX1
VcMATE1
AtALF5
SlMTP77
AtFFT
MtMATE2
NtMATE1
NtMATE2
AtTT12
MtMATE1
VvAM1
VvAM3
Consensus
RGLIPQLFAYAINFP+QRFLQAQSIVNPLAYISLG+LLLHILL+WLLVY+LGLGLLGAALAL
TM6
TM7
250
260
270
280
290
300
LaMATE2
VcMATE4
NtJAT1
AtDTX1
VcMATE1
AtALF5
SlMTP77
AtFFT
MtMATE2
NtMATE1
NtMATE2
AtTT12
MtMATE1
VvAM1
VvAM3
Consensus
SISWW+LVIALALYV+LSPSCKETWTGFSWEAF+GIW+FFRLSVASAVMLCLEIWYF+GLVL
D2
TM8
320
330
340
350
360
370
LaMATE2
VcMATE4
NtJAT1
AtDTX1
VcMATE1
AtALF5
SlMTP77
AtFFT
MtMATE2
NtMATE1
NtMATE2
AtTT12
MtMATE1
VvAM1
VvAM3
Consensus
LSGLLPNP+IA++SISICMNTNGWDYMIPLGL+AAASVRVSNELGAGHPRVAKFSV+VVVFL
D3

1020
1021

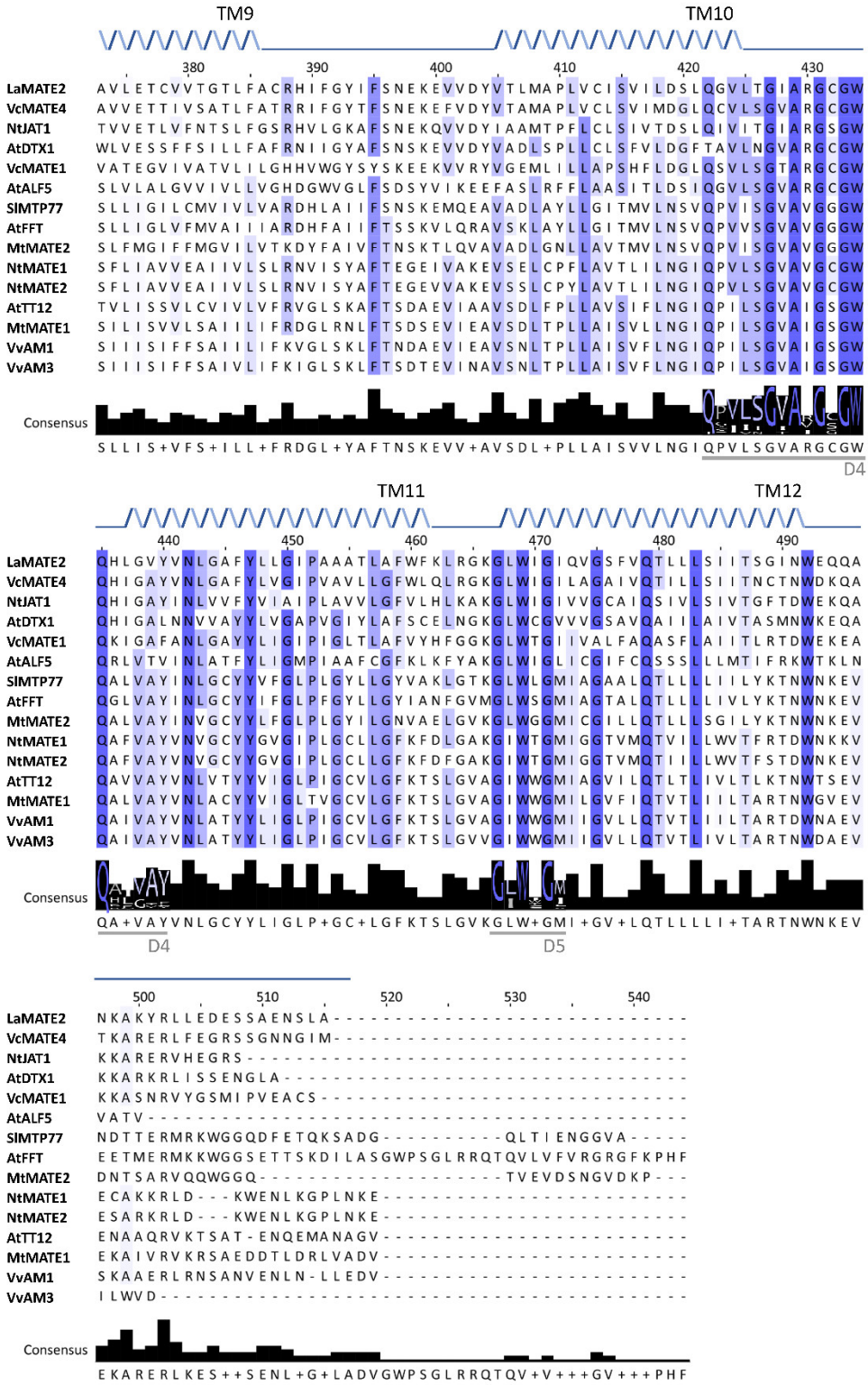
TM9
TM10
380 390 400 410 420 430
LaMATE2
VcMATE4
NtJAT1
AtDTX1
VcMATE1
AtALF5
SlMTP77
AtFFT
MtMATE2
NtMATE1
NtMATE2
AtTT12
MtMATE1
VvAM1
VvAM3
Consensus
SLLIS+VFS+ILL+FRDGL+YAFTNSKEVV+AVSDL+PLLAISVVLNGIQPVLSGVARGCGW
D4
TM11
TM12
440 450 460 470 480 490
LaMATE2
VcMATE4
NtJAT1
AtDTX1
VcMATE1
AtALF5
SlMTP77
AtFFT
MtMATE2
NtMATE1
NtMATE2
AtTT12
MtMATE1
VvAM1
VvAM3
Consensus
QA+VAYVNLGCYYLIGLP+GC+LGFKTSLGVKGLW+GMI+GV+LQTLLLLI+TARTNWNKEV
D4
D5
500 510 520 530 540
LaMATE2
VcMATE4
NtJAT1
AtDTX1
VcMATE1
AtALF5
SlMTP77
AtFFT
MtMATE2
NtMATE1
NtMATE2
AtTT12
MtMATE1
VvAM1
VvAM3
Consensus
EKARERLKES++SENL+G+LADVGWPSGLRRQTQV+V+++GV+++PHF

1022

1023 **Figure S3. Multiple sequence alignment of amino acid sequence**
1024 **of LaMATE2 with selected MATE transporter orthologs in**
1025 **higher plants**
1026 Protein sequence alignment was performed using Clustal-WS using
1027 Jalview software version 2 (Waterhouse *et al.,* 2009). Amino acids
1028 with only highly conservative substitutions are highlighted in colour
1029 blue. Thin grey lines below the consensus sequence (D 1-5) indicate
1030 five short stretches of conservative amino acids reported for all 56
1031 Arabidopsis MATE proteins. The red box indicates the residue E290
1032 (TT12), constituting the cation-binding site in the pore. Twelve
1033 putative-transmembrane helical domains (TM 1-12) of LaMATE2
1034 are indicated above the alignment
1035

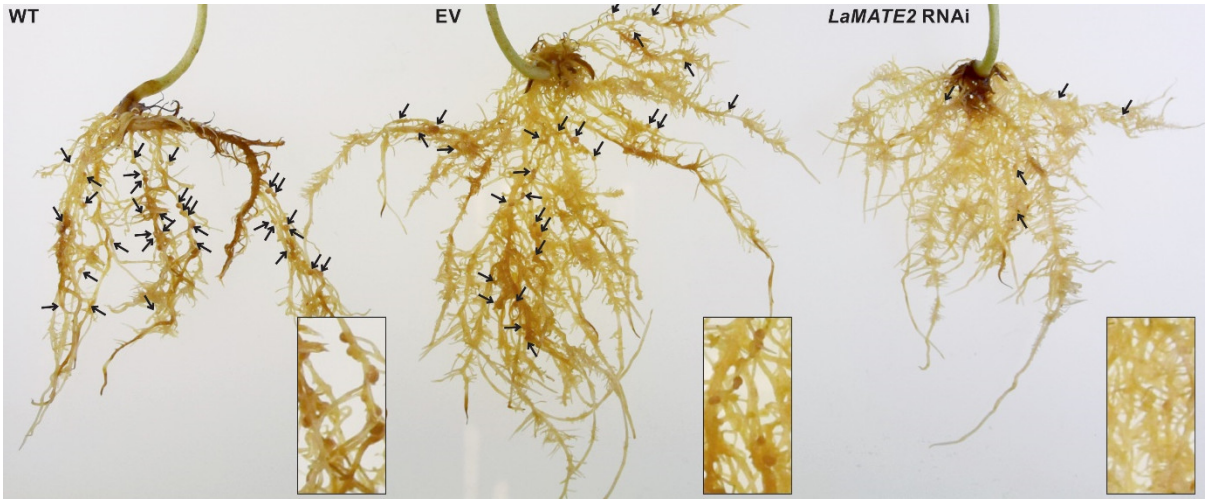


**Figure S4. Pictures of *LaMATE2*-silenced roots grown under N-deficient conditions**

Roots are shown in the following order: wild type, empty-vector-transformed roots and *LaMATE2*-RNAi-transformed roots. Nodule localizations are highlighted with arrows and close-up inserts are shown in the bottom right corners.

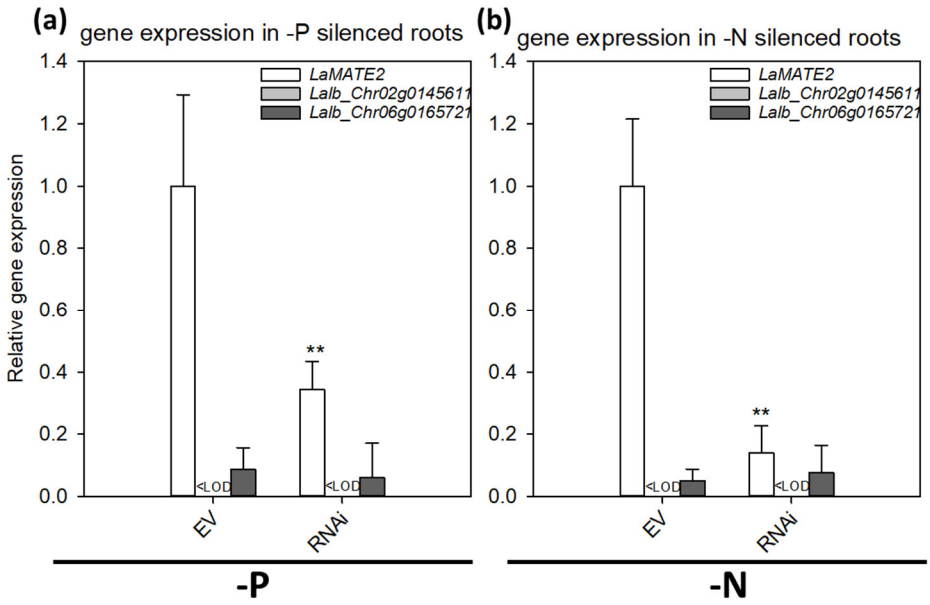


1047

1048 **Figure S5. Gene expression in the silencing experiments**

1049 Relative expression of *LaMATE2* and the two closest homologues:
1050 *Lalb_Chr06g0165721* and *Lalb_Chr02g0145611* in P-deficient (**a**)
1051 and N-deficient (**b**) condition in pRedRoot::*LaMATE2* RNAi
1052 (RNAi) or empty-vector pRedRoot (EV) transformed roots.
1053 Expression data are expressed relative to *LaMATE2* expression in
1054 EV-transformed roots. Data are means+SD (* refers to statistically
1055 significant differences among the mean value of RNAi and EV,
1056 ANOVA Holm–Sidak, N=3, **P <0.01).
1057

1058

1059 **Table S1.**

1060 List of primers

| | FORWARD | REVERSE |
|---|---|---|
| *LaMATE2* | cttgttttgctgtctgggct | tgcagcaccaattccaaagg |
| *LaIb_Chr06g0165721* | gtgaaacgatgaacatagaac | ctttgttgctgttgatgatg |
| *LaIb_Chr02g0145611* | agtgtcaacaccattgca | gatctaaccttgctgcag |
| *LaMATE2-GFP* | atagctagcatggaagagagtctaatacc | atacatgcctcatgctagactattttctgc |
| pNEV-*LaMATE2*ORF | atgcggccgcatggaagagagtctaatacc | agcggccgctcatgctagactattttctg |
| *LaMATE2* RNAi a | atccatggggcacgagatttctatct | gtgcatttaaatccacaaatagtttccagtc |
| *LaMATE2* RNAi b | atggatccccacaaatagtttccagtc | tgcactagtggcacgagatttctatct |
| *LaUbiquitin* | gcaccctagccgactacaac | ccggtaagggtcttgacaaa |

1061

1062

1063